DNA as a Programmable Viscoelastic Nanoelement

Richard A. Neher and Ulrich Gerland

Arnold Sommerfeld Center for Theoretical Physics and Center for Nanoscience, Ludwig-Maximilians Universität München, Munich, Germany

ABSTRACT   The two strands of a DNA molecule with a repetitive sequence can pair into many different basepairing patterns. For perfectly periodic sequences, early bulk experiments of Pörschke indicate the existence of a sliding process, permitting the rapid transition between different relative strand positions. Here, we use a detailed theoretical model to study the basepairing dynamics of periodic and nearly periodic DNA. As suggested by Pörschke, DNA sliding is mediated by basepairing defects (bulge loops), which can diffuse along the DNA. Moreover, a shear force f on opposite ends of the two strands yields a characteristic dynamic response: An outward average sliding velocity $v \sim 1/N$ is induced in a double strand of length N, provided f is larger than a threshold f_c. Conversely, if the strands are initially misaligned, they realign even against an external force $f < f_c$. These dynamics effectively result in a viscoelastic behavior of DNA under shear forces, with properties that are programmable through the choice of the DNA sequence. We find that a small number of mutations in periodic sequences does not prevent DNA sliding, but introduces a time delay in the dynamic response. We clarify the mechanism for the time delay and describe it quantitatively within a phenomenological model. Based on our findings, we suggest new dynamical roles for DNA in artificial nanoscale devices. The basepairing dynamics described here is also relevant for the extension of repetitive sequences inside genomic DNA.

INTRODUCTION

The basic double-helical structure of DNA is insensitive to the nucleotide sequence, but many of its biophysical properties are not. For instance, the local thermodynamic stability of double-stranded DNA (dsDNA) depends strongly on the sequence (1), and certain sequence motifs can cause permanent bends or make DNA more bendable (2). Such local modulations of the DNA properties play an important role in molecular biology, e.g., for nucleosome positioning (3) and transcription regulation through DNA looping (4). The sequence-dependent stability of DNA basepairing is also crucial for applications in nanotechnology (5–7). Clearly, since the thermodynamics of DNA basepairing is sequence-dependent, the kinetics is sequence-dependent as well. Our aim here is to show that the kinetics can display a much richer phenomenology than might be expected on the basis of the thermodynamics alone.

The dynamics of DNA basepairing can be probed experimentally on the single-molecule level with mechanical and optical techniques (8–14). One approach is to unzip dsDNA from one end of the double helix (12,13,15). However, unzipping probes only one aspect of the basepairing dynamics—the sequential opening of consecutive basepairs. In a different approach, a shear force is applied by grabbing the two strands on opposite ends of the dsDNA (16); see Fig. 1. For a heterogeneous dsDNA with a random sequence, the effect of a shear force is to unravel the basepairs from both ends (16); see Fig. 1 a, which is qualitatively similar to unzipping. In contrast, with a perfectly periodic sequence,

e.g., $(C)_N$ on the upper and $(G)_N$ on the lower strand or a higher-order repeat such as $(CA)_N$ and $(GT)_N$, the two strands can bind in many configurations (17). An applied shear force then facilitates local strand slippage and can induce macroscopic DNA sliding (18); see Fig. 1 b. (Throughout this article, we use the term ''DNA slippage'' for microscopic events where a few bases at the end of the double-strand unbind and rebind shifted by one or several repeat units. In contrast, ''DNA sliding'' refers to an average large-scale movement of the two strands against each other.)

DNA slippage is an aspect of DNA basepairing dynamics, which plays an important role in the generation of a class of genetic diseases (19,20). If local DNA slippage occurs in an Okazaki fragment during DNA replication, trinucleotide repeats inside genes can get extended beyond a threshold length for the onset of Huntington's and other diseases. Such slippage events are possible only within the time window that DNA polymerase needs to fill in the Okazaki fragment. Thus, the kinetics of strand slippage is an important determinant for the frequency of repeat extensions.

We propose that the dynamics of periodic and nearly periodic DNA is interesting also for the design of DNA-based nanodevices. Indeed, DNA is becoming increasingly popular as a building block for the assembly of nanoscale structures and devices (5–7). These applications already exploit the specificity of the basepairing interaction, e.g., to direct the assembly of DNA strands into predefined architectures, and the dynamics of DNA branch migration, e.g., to replace a bound DNA strand by a different strand. Below, in Discussion, we consider several new possible applications of DNA in nanotechnology, based on the dynamic properties identified in the main part of this article.

Finally, DNA sliding is interesting also from a purely theoretical perspective. Since simultaneous slippage of all basepairs is kinetically inhibited by an extensive activation barrier,
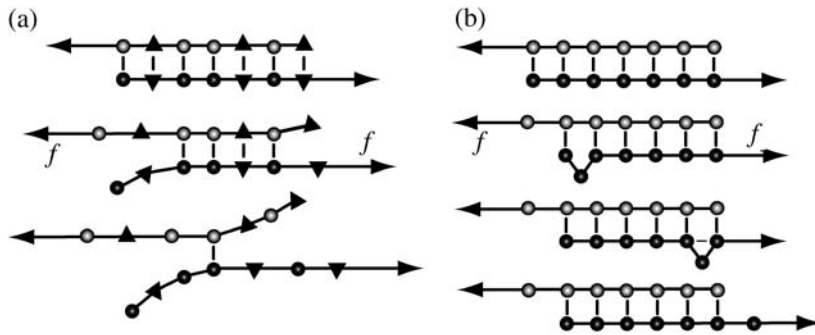
FIGURE 1 DNA under a shear force. (*a*) A nonperiodic sequence unravels from both ends, driven by the length gain from converting stacked bases into longer single strands. (*b*) A periodic DNA sequence can open by sliding, mediated by bulge loops that are created at the ends and diffuse freely along the DNA. When a bulge loop reaches the opposite end, the two strands have effectively slipped against each other by a distance equal to the loop size.

the macroscopic sliding of DNA strands is a complex process involving the dynamics of many local basepairing defects (17,18). The most likely defects are bulge loops (see Fig. 1 *b*), which are created at the ends of the dsDNA, or, in pairs, anywhere along the molecule. Once formed, bulge loops diffuse freely along a periodic dsDNA until they annihilate with a loop on the opposite strand or are absorbed at an end. Mutations in the periodicity of the DNA sequence create obstacles for the diffusion of bulge loops. Effectively, the bulge-loop dynamics can be regarded as a reaction-diffusion process of particles and antiparticles in one dimension. DNA shearing experiments render certain aspects of these dynamics observable and permit a quantitative characterization.

The outline of this article is as follows. First, we describe our theoretical model for the energetics and dynamics of DNA basepairing under a shear force. We then show that our model leads to the following predictions:

1. For periodic dsDNA, the combination of polymer mechanics and basepairing dynamics gives rise to a viscoelastic response to shear forces above a threshold f_c, where both f_c and the viscosity η are programmable over a wide range through the DNA sequence. The viscoelastic behavior can be described with the help of a mechanical analog model.
2. DNA sliding is possible even when the exact sequence periodicity is destroyed by a few mutations.
3. The mutations affect the viscoelastic behavior by introducing a programmable time delay before sliding commences after a sudden force jump.
4. The mechanism for the time delay can be understood within a phenomenological model, which also permits a quantitative description of the full distribution of time delays. Taken together, we find that the sequence dependence of the basepairing dynamics allows us to adjust the mechanical response of DNA under a shear force over a broad range of behaviors. In the last section, we discuss the experimental ramifications of these findings.

DNA MODEL

To study the dynamics of DNA sliding, we consider a DNA molecule under a shear force f, which can be applied experi-

mentally by pulling the opposite 5′ ends (16) or, alternatively, the opposite 3′ ends. In a coarse-grained description, the configuration of the DNA is specified by its basepairing pattern S and the spatial contours of both strands. A generic configuration consists of two stretched and two unstretched single strands, and the central region from the first to the last basepair (see Fig. 1).

We will not explicitly describe the dynamics of the spatial polymer degrees of freedom, but assume rapid equilibration compared to the timescale of DNA sliding. This assumption is justified for short DNA molecules: The timescale to equilibrate a semiflexible polymer of length L and persistence length l_p in a solvent of viscosity η is $\eta L^4/72\,l_p^2 f$, where f is an external force applied to its ends (21). For a DNA of 150 bp (one persistence length) in water at a 10-pN load, the equilibration time is on the order of 0.01 μs, which is fast compared to the millisecond timescale of DNA sliding observed in the reannealing experiments of Pörschke (17). Hence, we integrate out the contour conformations to obtain a free-energy function $E(S)$ that depends only on the basepairing pattern S. The total free-energy $E(S)$ can be split up into three terms,

$$E(S) = E_{stretch}(S) + E_{bp}(S) + E_{loop}(S), \qquad (1)$$

corresponding to the stretching energy, the free-energy gain due to basepairing, and the free-energy cost of (internal or bulge) loops in the pattern S, respectively.

Polymer model

The mechanical polymer properties of DNA enter only into the stretching energy, which we write in the form $E_{stretch}(S) = -f L(S)$, with an effective force-dependent total length $L(S)$ for the stretched DNA, i.e., the two single-stranded ends where the force is applied and the central DNA segment from the first to the last basepair (see Fig. 2). The unstretched single strands do not contribute to the free energy, since we take all energies relative to the unstretched and unpaired state, which is the usual convention (1). For the stretched single strands, we use a freely jointed chain polymer model with a Kuhn length twice the bare segment length $b_s \approx 0.7$ nm for a single base (22). With this model, each unbound
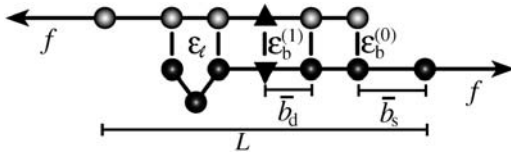
FIGURE 2 DNA free-energy model. The free energy $E(S)$ of a basepairing pattern S contains three separate contributions: first, a negative binding energy for basepairing. For simplicity, we assign the same binding energy $\varepsilon_b^{(k)}$ for every basepair of type k, regardless of the neighboring bases. Second, a positive free energy cost for internal and bulge loops. We assign the same cost ε_ℓ for every loop, regardless of its length and base sequence, since the detailed choice of the loop cost function does not affect our main findings. Third, a stretching energy. For a given pattern S, the stretching energy can be written in the form $-f L(S)$, with an effective length $L(S)$, which is obtained from force-dependent base-to-base distances $\bar{b}_d(f)$ and $\bar{b}_s(f)$ for double and single strands, respectively. Note that $L(S)$ does not correspond to the physical length of the DNA molecule (see main text).

base at the ends where the force is applied contributes an effective length $\bar{b}_s(f)$ to the total length $L(S)$, where

$$\bar{b}_s(f) = -\frac{k_B T}{2f} \ln\left(\frac{\sinh(2fb_s/k_B T)}{2fb_s/k_B T}\right) \tag{2}$$

and $k_B T$ is the thermal energy. Note that $\bar{b}_s(f)$ differs from the average extension of one segment in the direction of the force. Instead, the average total extension $\langle x \rangle$ of a DNA with basepairing pattern S is calculated as the force derivative of the stretching free energy,

$$\langle x \rangle = \frac{\partial E_{\text{stretch}}(S)}{\partial f}, \tag{3}$$

which yields the correct (Langevin) form for the extension of a freely jointed chain. For the central DNA region from the first to the last basepair, we assume a B-DNA conformation and use a wormlike-chain model with persistence length $l_p = 50$ nm and a contour length of $b_d = 0.34$ nm per base. (The length of an asymmetric loop in the central region is approximated by counting only the bases in the shorter arm of the loop.) For the forces of interest here, the effective length of a basepair, $\bar{b}_d(f)$, is given by the asymptotic formula

$$\bar{b}_d(f) = b_d\left(1 - \sqrt{\frac{k_B T}{4 f l_p}}\right). \tag{4}$$

The force-dependence of the lengths $\bar{b}_s(f)$, $\bar{b}_d(f)$ is, in fact, essential only for our calculation of the viscoelastic response. For all other properties considered below, the force-dependence has no qualitative effect, and will hence be neglected (i.e., $\bar{b}_s(f) = b_s$, $\bar{b}_d(f) = b_d$ everywhere except in Viscoelastic Behavior).

Basepairing energy model

To obtain a compact theoretical description, we use a basepairing energy model which is simplified from the nearest-neighbor model of SantaLucia (1), but nevertheless permits

semiquantitative predictions. We exclude basepairs within a strand, and assign a binding (free) energy $\varepsilon_b^{(k)} > 0$ for each basepair of type k (Watson-Crick or other) between strands (see Fig. 2). Hence, $E_{bp}(S) = -\Sigma_k n_k(S)\varepsilon_b^{(k)}$, where $n_k(S)$ is the total number of type k basepairs in the basepairing pattern S. Similarly, we assign a loop initiation cost $\varepsilon_\ell > 0$ for each internal or bulge loop in a given pattern (we neglect an additional length-dependent loop cost, which has no qualitative effect on the results discussed below). Therefore, $E_{\text{loop}}(S) = q(S)\varepsilon_\ell$, where $q(S)$ is the total number of loops in the pattern. The numerical values of the free-energy parameters $\varepsilon_b^{(k)}$ and ε_ℓ are temperature-dependent (1). The actual values used in our simulations are given below.

Elementary kinetic steps

We support our phenomenological theory presented below by simulating the DNA basepairing dynamics in detail. To this end, we use a kinetic Monte Carlo scheme with three single base moves as elementary steps (23): basepair opening, basepair closing, and basepair slippage. Here, basepair slippage refers to a local shift of the binding partner of a base, which is possible only for basepairs next to unbound bases, i.e., inside loops or at the ends of the molecule. Clearly, basepair slippage can also be generated by a basepair opening move followed by a basepair closing move. However, the work of Pörschke (17) indicates that basepair slippage is faster than would be expected from the individual rates for basepair opening and closing (see below). Hence, we include the basepair slippage move, as has been done previously (23).

Kinetic rates

To fully specify our model for the DNA basepairing dynamics, we need to assign a rate to each elementary kinetic step. Careful relaxation experiments (24) determined the rate for basepair closing at the end of helical segments to be $1–20 \times 10^6$ s^{-1}, where the range indicates the experimental uncertainty. In our model, we assume that this rate is independent of the identity of the basepair. To reproduce the correct equilibrium behavior from our basepairing dynamics, the rate for opening a basepair of type k at the end of a helix must be reduced by a factor $\exp(-\varepsilon_b^{(k)}/k_B T)$ with respect to the closing rate. From reannealing experiments with periodic sequences, Pörschke (17) estimated the rate for the displacement of a bulge loop by one base, i.e., the rate for basepair slippage, to be $\sim 5 \times 10^6$ s^{-1}. Hence, the rates for basepair closing and basepair slippage are approximately equal, within experimental accuracy. In our model, we set them exactly equal, for simplicity (our main results are, in fact, insensitive to the precise value of the closing rate; see below). In general terms, our model assumes that all kinetic rates of passing from a higher energy configuration to one with lower energy are the same, whereas the reverse rates are chosen to obey detailed balance. It may be noteworthy that

recent theoretical work on the kinetics of force-induced RNA unfolding, which used similar assumptions, produced surprisingly good agreement with experiment (25).

Below, we report all of our kinetic simulation data in units of Monte Carlo steps. From Pörschke (17), our best estimate for the real-time equivalent of one Monte Carlo step is 0.2 μs. However, it should be kept in mind that this estimate beares a large uncertainty.

SLIDING DYNAMICS OF PERIODIC SEQUENCES

The simplest periodic sequence is a repetition of one base on one strand, e.g., AAA. . ., and the complementary base on the other. In this case, we have only basepairs of one type (i.e., $\varepsilon_b^{(k)} \equiv \varepsilon_b$ in our model) and each base on one strand can bind to any base on the other strand. For longer repeat units, e.g., triplet repeats such as CAGCAG. . ., which play an important role in genetic diseases (19), one can treat a repeat unit as an effective base with larger associated energies ε_b, ε_ℓ and lengths b_d, b_s. We are interested in the basepairing dynamics induced by a constant shear force f that is suddenly turned on at $t = 0$. In the following, we first review the physical description of DNA sliding dynamics, which we have established already in Neher and Gerland (18). We then construct a mechanical analog model to characterize the viscoelastic response of periodic DNA and its sequence-dependence.

Quantitative phenomenological description

As illustrated in Fig. 1 b, sliding of periodic dsDNA is mediated by the creation, diffusion, and annihilation of bulge loops. When a force is applied, the diffusion of bulge loops within the dsDNA remains unbiased, assuming the force does not deform the dsDNA structure significantly (this assumption clearly breaks down for forces above the B-S transition around 65 pN). In contrast, the force strongly affects the rates at which bulge loops are created at the ends. When the two DNA strands are misaligned, these creation rates are imbalanced, since a bulge at an overhanging end does not reduce the number of basepairs in the structure (although it does on the opposite end). This imbalance produces a restoring force f_c, which can be obtained approximately (18) by balancing the energy cost of breaking a basepair with the gain in stretching energy, $\varepsilon_b = f \times (2\,\bar{b}_s(f) - \bar{b}_d(f))$. The restoring force creates an average inward drift that realigns the two strands. To obtain an outward drift velocity v, i.e., macroscopic sliding, one needs to overcome the restoring force f_c, so that $v \sim (f - f_c)$ in the vicinity of f_c. Indeed, f_c becomes a critical force in the thermodynamic sense when the limit of a large strand length N is taken and the state where the strands are completely separated is excluded.

At the critical force, the rates at which bulge loops are produced are equally large on the overhanging stretched and the unstretched ends. The average sliding velocity v van-

ishes; however, the bulge-loop dynamics still leads to a macroscopic diffusion of the two strands relative to each other, with a diffusion coefficient D. Interestingly, this diffusion coefficient scales with the total number of bases as $D \sim 1/N$, so that the rupture-time τ required to separate the two strands completely scales as $\tau \sim N^3$ instead of the usual $\tau \sim N^2$ for diffusion of a particle over a distance N. This scaling of D is due to the fact that loops are generated at the ends with a constant rate, but only result in a global shift between the strands, if they diffuse over a distance $\sim N$, either to annihilate at the other end or with a loop on the opposite strand. In both cases, the probability for an event scales as $1/N$. The $D \sim 1/N$ scaling occurs also in the reptation problem of polymer physics, and indeed the microscopic origin is closely related, as motion is mediated by defect diffusion (26).

Since the production of a loop on the stretched ends shortens the molecule, the corresponding production rate decreases with f. Hence, the rates of events extending or shortening the double-stranded region, that are equal for $f = f_c$, differ at other forces resulting in a drift. Each of these rates, and consequently the sliding velocity v as well, is proportional to $1/N$. From the Einstein relation, one expects $v \sim (f - f_c)D \sim 1/N$, in agreement with this result. With the negative (inward) drift velocity below f_c, rupture events are driven by rare fluctuations, and the rupture-time τ grows exponentially with N, as is characteristic for thermally activated transport over an extensive energy barrier. On the other hand, for forces larger than f_c, the N^{-1} scaling of v leads to rupture times increasing as $\tau \sim N^2$.

This scaling holds up to a force f^*, above which the rupture times grow only linearly with N, due to a dynamical transition in the opening mode from sliding to unraveling (i.e., the opening mode of heterogeneous dsDNA). For $f > f^*$, it is energetically favorable to break basepairs consecutively from both ends and both strands are separated after breaking N basepairs. Within our model, f^* is well approximated by the solution of $f = \varepsilon_b/[\bar{b}_s(f) - \bar{b}_d(f)]$—i.e., the balance between the basepairing energy and the stretching energy gained by extending the molecule by the difference between the length of an unbound base and a basepair. (For DNA sequences where this force is large enough to deform the DNA structure, in particular for f^* above the $\sim$65 pN of the B-S transition, the unraveling mode may not exist.)

Viscoelastic behavior

DNA sliding can be regarded as a viscous flow of the two strands relative to each other. According to the physical picture reviewed above, this flow has interesting nonlinear and sequence-dependent properties. Since the shear force also elicits an elastic response (due to the entropic elasticity of DNA), the behavior of periodic dsDNA is reminiscent of a viscoelastic material. Such materials combine solidlike and fluidlike mechanical properties when probed by external stress. In the following, we examine this analogy more closely.

The mechanical behavior of a typical viscoelastic material can be described by a Zener model (27), which is constructed, e.g., by connecting a Kelvin element (a dashpot in parallel with a spring) in series with a spring (see Fig. 3). The Zener model reproduces the two prominent characteristics of viscoelastic materials:

1. In a creep experiment, where a constant stress is suddenly applied, an instantaneous elastic strain is followed by a gradual creep toward a new equilibrium.
2. When the strain is suddenly increased, the stress rises sharply and then relaxes gradually to an equilibrium value.

On a qualitative level, periodic dsDNA displays these same characteristics in its average behavior:

1. Upon sudden application of a constant force f in the range $f_c < f < f^*$, the DNA rapidly stretches against its entropic elasticity and slowly creeps with a viscosity η that is proportional to the number of bases in the double strand. However, it will not approach a new equilibrium, but eventually rupture.
2. When the extension of the DNA is suddenly increased, the tension rapidly rises and then slowly relaxes to the critical value f_c (provided the initial rise was above f_c).

The viscoelastic behavior of periodic DNA can be described by a nonlinear generalization of the Zener model (see Fig. 3 b), where the Kelvin element effectively describes the basepairing dynamics, while the outer elastic element accounts for the entropic elasticity of the polymer backbone (consisting of dsDNA, single-stranded DNA, i.e., ssDNA, and, if present, linkers to the points of force application). Since the basepairing dynamics of two misaligned complementary periodic DNA strands produces a restoring force f_c, the sliding velocity v is proportional to $f - f_c$. The sliding dynamics is thus described by a dashpot in parallel with

a potential generating the restoring force and preventing contraction beyond maximal overlap. In contrast to the standard Zener model with harmonic springs, the stress in response to a strain will relax to the value f_c, independent of the displacement (within a certain range). Fig. 3 a shows extension-time-traces obtained from our model, both for a periodic (*bottom panel*) and a heterogeneous DNA (*center panel*); see Fig. 3 legend for parameters. Here, we have considered a creep test situation where the force is switched periodically between $f_{min} < f_c$ and $f_{max} > f_c$ (*top panel*). Fig. 3 c shows the corresponding behavior of the generalized Zener model for comparison. We observe that the average behavior of the periodic DNA resembles that of the generalized Zener model, whereas the heterogeneous DNA shows only elastic behavior. Of course the extension also displays strong thermal fluctuations, which play an important role in single-molecule dynamics, and ultimately lead to rupture even below the critical force (18).

Programmability

The viscoelastic behavior described above relies on the basepairing dynamics within the DNA molecule, and is manifestly sequence-dependent. This fact makes the mechanical behavior of dsDNA under shear-force programmable, i.e., both the force offset f_c and the viscosity η can be adjusted through sequence composition and length of the dsDNA. Even for perfectly periodic sequences, there is still a considerable freedom in the choice of the sequence composition, since a repeat unit can be several bases long and involve different combinations of Watson-Crick and other basepairs. Exploiting this freedom, the range over which the average basepairing energy ε_b can be programmed is ~ 0.5–$4\ k_BT$ (1), which translates into an equally wide range of force offsets $f_c = \varepsilon_b/(2\bar{b}_s - \bar{b}_d)$. (The precise experimental range of the force offset is difficult to predict,
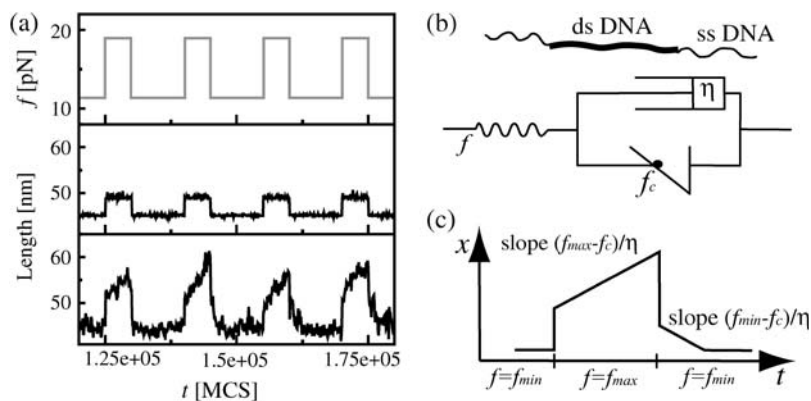
FIGURE 3 Viscoelastic response of periodic DNA. (*a*) The shear force on an 80-bp dsDNA (with two 20-bp ssDNA linkers) is switched periodically between $f_{min} = 11.4$ pN and $f_{max} = 19$ pN (*upper panel*). The center and bottom panels show the extension-time-trace for heterogeneous and periodic DNA, respectively (energy parameters: $\varepsilon_b = 1.11\ k_BT$ and $\varepsilon_\ell = 2.8\ k_BT$, roughly corresponding to AT basepairs at 50°C (18)). The time units are Monte Carlo steps, the real-time equivalent of which is discussed in Kinetic Rates (see article). The heterogeneous DNA responds only elastically to the force jumps, mostly due to stretching of the linkers. The length of the periodic DNA shows a similar elastic strain, but in addition, the molecule elongates at a finite speed due to sliding, since $f_{max} > f_c = 16.3$ pN. When the molecule is relaxed, we find an elastic response and inward sliding, since $f_{min} < f_c$. The length of the periodic DNA fluctuates strongly due to loop formation and annihilation. (*b*) The viscoelastic behavior displayed by a periodic DNA molecule can be described by a generalized Zener model, where harmonic springs are substituted by anharmonic elastic elements describing polymer elasticity and the restoring force f_c. The ideal dashpot (with viscosity η) creates the viscous behavior of periodic dsDNA. (*c*) The response of the above idealized model to the same periodic force resembles the average response of periodic DNA.

since it depends sensitively on the effective ssDNA and dsDNA length. Roughly, we expect values of up to 30 pN.)

The velocity of macroscopic strand sliding is determined by four factors: 1), the mobility of defects, i.e., the rate for bulge-loop displacement; 2), the bulge-loop density; 3), the inverse strand length; and 4), the deviation of the force f from the critical force f_c. The defect density depends sensitively on the basepairing free energy and may vary roughly between 0.001 and 0.2 for different repeat lengths and temperatures, leaving great freedom to adjust the timescale of DNA sliding. Note that since only the bulge-loop density and not the individual rates for basepair closing and opening influence the sliding velocity, the rate for bulge-loop displacement is the only crucial rate parameter in our model. By increasing the strand length, the sliding velocity can be made arbitrarily small, or, equivalently, the viscosity η can be made arbitrarily large ($\eta \sim N$). Alternatively, η is increased by using longer repeat units, since η grows exponentially with the free energy cost of creating a bulge loop. An order-of-magnitude estimate for the lower bound on η yields $\sim 10^{-3}$ pN $\times$ s/nm, based on reannealing experiments with homogeneous oligonucleotides of 10 bps (the reannealing experiments of Pörschke (17) suggest that a misaligned 10-bp molecule can slide by one basepair within 0.1 ms; assuming that the sliding velocity extends linearly from $f_c \sim 10$ pN to force zero, one obtains the estimate $\eta \sim 3 \times 10^{-3}$ pN $\times$ s/nm). With these force- and timescales, DNA sliding should be well observable in single-molecule experiments.

PERIODIC DNA WITH WEAK SEQUENCE DISORDER

How is the basepairing dynamics affected when a few mutations destroy the perfect periodicity? Fig. 4 (*top*) shows two simulated extension-time-traces, one for a perfectly periodic sequence and one with $M = 7$ equidistant mutations (DNA parameters; see Fig. 4's legend). Here, we assigned the same binding energy to mutated and original basepairs, to focus on the effects that mutations exert on the basepairing dynamics rather than the energetics. Furthermore, we assumed that mutated bases can only bind to their ground-state binding partners, i.e., mutated bases cannot form basepairs with the original bases and all mutations are of a different type. The less generic effects that can result without these assumptions are discussed below.

We observe that the mutations have a drastic effect: whereas the original sequence begins to slide almost immediately after application of the force, the mutated sequence exhibits a pronounced delay before sliding sets in. Indeed, the figure suggests that the mutated sequence has two characteristic timescales: a waiting time τ_w, during which the extension fluctuates around a constant value; and a sliding time τ_s, during which the extension increases until the two strands are completely separated. Another, less drastic effect of the mutations is to reduce τ_s; i.e., once sliding starts, it is
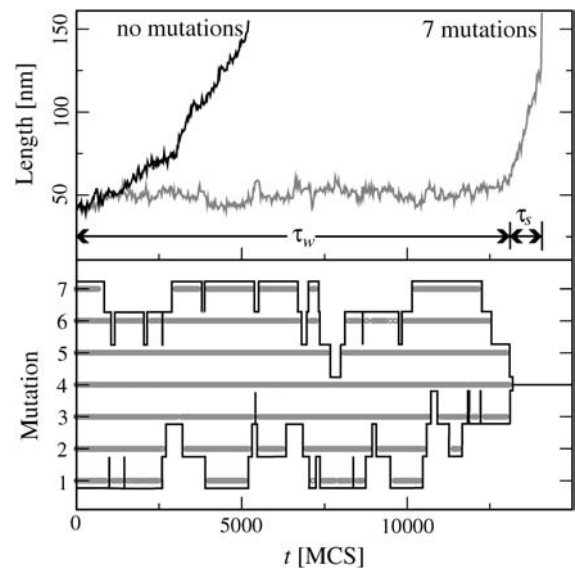

FIGURE 4 (*Top*) Extension-time-trace for a perfectly periodic DNA of $N = 120$ basepairs and the same DNA with seven mutations, both under a shear force of $f = 12.7$ pN (energy parameters as in Fig. 3). Whereas the molecule without mutations starts sliding almost immediately, the molecule with mutations fluctuates about its initial length for some time τ_w before sliding starts. (*Bottom*) The time-trace of the binding state (open/closed) for the seven mutated basepairs in the sequence. Each mutated basepair (1–7) is unbound wherever the corresponding thick horizontal line is broken, and bound where the line is shown. Note that the mutated basepairs do not open/close independently from each other. Instead, a mutated basepair opens only once all mutated basepairs to the left or right are already open. The black envelope curves emphasize the positions of the outermost bound mutation on each side. Their dynamics resembles a (biased) random walk. Sliding begins when all mutations are open.

faster than without mutations. Note that the convex shape of both sliding curves is due to the fact that the sliding velocity increases as the length of the double-stranded region decreases, $v \sim \eta^{-1} \sim N^{-1}$ (see above).

What is the physical mechanism that sets the waiting timescale (τ_w)? Clearly, sliding can begin only after all mutated basepairs have been broken, since otherwise the two strands are locked into one relative position. Arguably the simplest scenario would be that all mutations independently fluctuate between the open and closed states, and sliding commences when all mutations happen to be open simultaneously. Alternatively, the dynamics of the mutated basepairs could be correlated. To clarify the dynamical mechanism, we plotted the binding state (bound/unbound) of all mutated basepairs alongside the trajectories in Fig. 4 (*bottom, shaded curves*). It is evident that the mutations do not open independently. Instead, interior mutations open only once the neighboring mutation toward the exterior has already opened.

The two-random-walkers model

Inspection of Fig. 4 (*bottom*) suggests that the positions of the two outermost-bound mutations might, in fact, perform
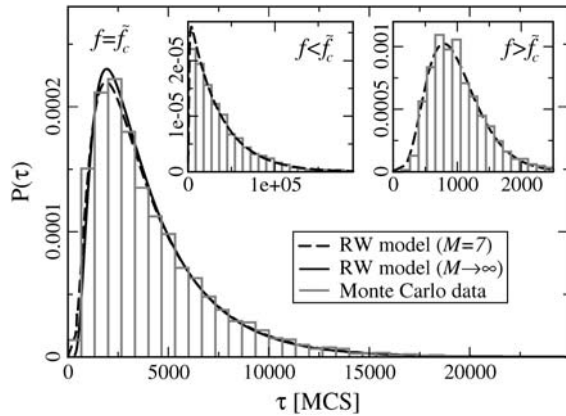
FIGURE 5 Waiting time distributions. (*Main panel*) The histogram of waiting times τ_w of a 120-bp-long DNA sequence with $M = 7$ equidistant mutations subject to a force $f = \tilde{f}_c = 12.9\text{pN}$, is well described by the distribution of collision times (*dashed line*) of the two-random-walker model (see main text and Fig. 6). The solid line shows the parameter-free asymptotic distribution of Eq. 5 for comparison. (*Insets*) Distribution of τ_w for forces above and below $\tilde{f}_c$ ($f = 15.2$ pN and $f = 11.4$ pN, respectively). The dashed lines are fits using the RW model with directional bias (see main text).

a (biased) random walk (see the *black curves* in Fig. 4). If true, the waiting time τ_w could be interpreted as the first collision time τ_c of two random walkers (2RW) on a row of $M + 1$ discrete sites, with force-dependent in- and outward hopping rates k_{in} and k_{out}. To test this hypothesis, we compare the histogram of τ_w values (from many simulations) with the distribution $P(\tau_c)$ of first collision times for 2RW. Fig. 5 shows three such histograms (*main panel* and *two insets*) obtained with the same DNA parameters as in Fig. 3, but with three different forces. Superimposed are the distributions $P(\tau_c)$, calculated as described below and in Supplementary Material. The case shown in the main panel of Fig. 5 corresponds to a force value for which the 2RW are unbiased—i.e., $k_{in} = k_{out}$—whereas the left inset corresponds to a smaller force producing a bias to the outside ($k_{out} > k_{in}$) and the right inset shows the opposite case of a larger force and $k_{out} < k_{in}$. In all three cases, the observed histogram is well described by the 2RW model. Indeed, despite some caveats (see below), this model can serve as a useful coarse-grained description for the basepairing dynamics preceding the sliding stage.
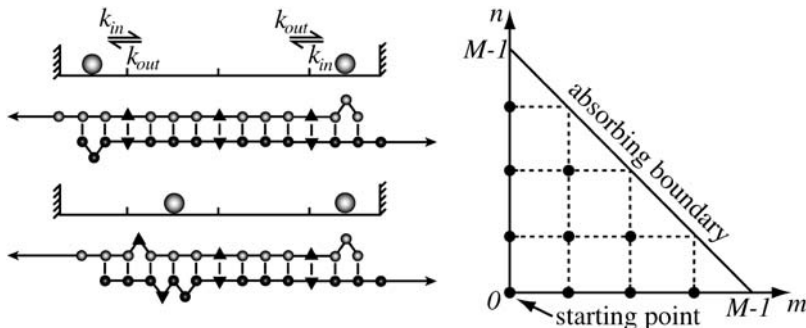
The calculation of the first collision time distribution $P(\tau_c)$ belongs to the class of first-passage problems, which has been studied extensively in statistical physics (28). In the context of the helix-coil transition, Schwarz and Poland (29) (see also (30)) already solved the associated diffusion problem. Here, we use their work as a basis to treat the first-passage problem. One can replace the problem of 2RW in one dimension by the equivalent problem of one RW on a two-dimensional lattice with a triangular shape (see Fig. 6). In the following, the unbiased case ($k_{in} = k_{out} \equiv k$) is of particular interest. In this case, there is only the single rate constant k, which can be absorbed in the unit of time, so that the distribution $P(\tau_c)$ depends only on the number of lattice points (i.e., the number of mutations). However, in the limit of large M this dependence also disappears, if we use the rescaled collision time $\tilde{\tau}_c = \tau_c k/M^2$. The resulting parameter-free distribution can be expressed in the form (see Supplementary Material) of

$$P(\tilde{\tau}_c) = -\frac{16}{\pi^2} \frac{\partial}{\partial t}[Q(t)]^2|_{t=\tilde{\tau}_c}, \quad (5)$$

where $Q(t)$ is the rapidly converging series

$$Q(t) = \sum_{n=1}^{\infty} \frac{(-1)^n}{2n-1} \exp\left(-\frac{\pi^2}{2}(2n-1)^2 t\right). \quad (6)$$

This distribution is plotted as the solid line in the main panel of Fig. 5. Even when M is small, it is a good approximation to the actual distribution, as illustrated by the dashed line in Fig. 5 showing the exact distribution for the case of $M = 7$.

In the case of biased RW ($k_{in} \neq k_{out}$), we compute $P(\tau_c)$ numerically. The dashed curves in the insets of Fig. 5 show these distributions for $M = 7$ mutations, where we have used the rates k_{in}, k_{out} as fit parameters.

Scaling of mean waiting time

In the 2RW model, the mean first collision time follows the diffusive behavior $\tau_c \sim M^2$ when the RW are unbiased (see above). When the walkers have an inward bias, this changes to linear scaling $\tau_c \sim M$, whereas τ_c increases exponentially with M for an outward bias (see Supplementary Material). To test these predictions of the 2RW model, we determined the

FIGURE 6 On a coarse-grained level, the dynamics of mutation opening/closing can be described by a model of two particles hopping on a one-dimensional lattice, with inward/outward hopping rates k_{in}, k_{out}. Their positions represent the two outermost closed mutations. When the particles collide, all mutations have opened. Equivalently, one can consider a single particle hopping on a triangular two-dimensional lattice. The first collision time then corresponds to the time to reach the diagonal absorbing boundary.

mean waiting time $\langle \tau_w \rangle$ for different M and different forces f from our DNA simulations. Fig. 7 a shows $\langle \tau_w \rangle$ as a function of M (on a double logarithmic scale) for the same three force values as in Fig. 5. Here, we increased the total DNA length N proportional to M, to keep the mutation density constant and equal to that of Fig. 5. At the smallest force, the waiting time increases exponentially with M, as expected. At the intermediate force, corresponding to the case of unbiased walkers, we find a scaling $\langle \tau_w \rangle \sim M^\zeta$ with $\zeta \approx 2.4$, while $\zeta \approx 1.5$ for the largest force. We expect that the values of these exponents are strongly influenced by finite size effects, since we can vary M only over roughly one decade. However, our results indicate that the waiting times increase more rapidly with the system size than expected on the grounds of our phenomenological 2RW model. A possible explanation is given in Microscopic Mechanism, below.

How does the mean waiting time depend on the applied force? Fig. 7 b shows three curves of $\langle \tau_w \rangle$ versus f for

different mutation densities. The vertical dashed lines indicate the force value where $k_{in} = k_{out}$ for each curve. Below these values, $\langle \tau_w \rangle$ increases sharply with decreasing force. Indeed, it is reasonable to consider the force $\tilde{f}_c$ where $k_{in} = k_{out}$ as a generalization of the critical force f_c to the case of weakly disordered sequences. As explained in Supplementary Material, the rates k_{in}, k_{out} can be extracted in several different ways from the simulation data, leading to $\tilde{f}_c$ values which are mutually compatible.

Fig. 7 c summarizes the different dynamical regimes as a function of the applied force f and the mutation density ν. Without mutations ($\nu = 0$) the force axis is divided into three regimes, with rupture driven by rare fluctuations, continuous sliding, and unraveling at low, intermediate, and large forces, respectively. As mutations are introduced ($\nu > 0$), the boundary $\tilde{f}_c(\nu)$ between the fluctuation-driven Kramer's regime and the sliding regime rises to larger forces, and the sliding regime acquires the time delay of Fig. 4 as a new feature. It is clear from Fig. 7 c that the force interval displaying sliding behavior becomes narrower as the mutation density is increased. This trend can be understood within a more microscopic picture (see below). We could not determine unambiguously whether the sliding regime vanishes completely already at a finite mutation density. However, it is clear that sliding will, in practice, be unobservable for sequences with many mutations. The qualitative features depicted in Fig. 7 c are robust against variations in our microscopic parameters ε_b, ε_ℓ, $\bar{b}_s(f)$, and $\bar{b}_d(f)$. However, the positions of the boundaries between the different regimes depend on these parameters (see below).

Microscopic mechanism

Why does the mutation dynamics of Fig. 4 (*bottom*) resemble the behavior of two random walkers? First, the opening of a mutation (and subsequent local shift of the two strands against each other) is always associated with the formation of two permanent loops (see Fig. 6, *left*). Hence, the opening of mutations is energetically expensive and mutations remain mostly closed, as long as this cost is not compensated by any gain in entropy or stretching energy. Since there is no such gain when an interior mutation opens, mutations can only open beginning from the ends toward the inside: loops are constantly created at the ends of both strands and propagate inwards until they hit a mutation, which forms a barrier to bulge-loop diffusion. On the unstretched strand, loops are generated at a higher rate than on the stretched strand, resulting in a larger quasi-equilibrium loop density (18). When the outermost bound mutation opens spontaneously, the accumulated loops on the exterior unstretched strand can suddenly penetrate to the inside. This penetration results in an entropy gain and a relative shift of the mutated bases, which prevents immediate recombination (see Fig. S10 in Supplementary Material). The size of the entropy gain and the shift
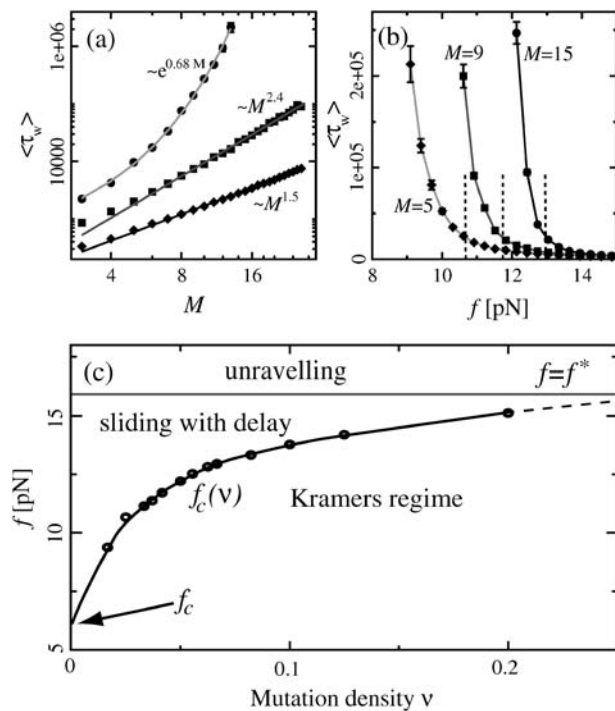
FIGURE 7 (*a*) The mean waiting time $\langle \tau_w \rangle$ as a function of the system size (the mutation density of $\nu = 1/15$ is kept fixed as the number of evenly spaced mutations M is increased). At low forces the scaling is exponential (*circles*, data for $f = 11.4$ pN; *solid line*, exponential fit), while we find power-law behavior at the force threshold ($\tilde{f}_c = 12.9$ pN, *squares*) and above ($f = 15.2$ pN, *diamonds*). (*b*) The mean waiting time as a function of the applied force for a sequence of $N = 240$ bp with 5, 9, and 15 mutations. The dashed lines indicate the threshold force $\tilde{f}_c$ for each case. Below the threshold, $\langle \tau_w \rangle$ rises sharply. (*c*) Different regimes of the DNA dynamics in the parameter space (f, ν). The Kramers regime (DNA rupture becomes exponentially slow with increasing system size) is separated from the (delayed) sliding regime by the line $\tilde{f}_c(\nu)$ where the inward and outward hopping rates are equal, $k_{in} = k_{out}$ (*circles*, data; *solid line*, interpolation). At forces larger than f^*, the molecule dissociates by unraveling from both ends.

increases with the distance to the next mutation. Therefore, the mutation density, not the absolute number, is the relevant parameter that determines the relative magnitude of the hopping rates k_{in} and k_{out} in the random-walker model, and hence fixes the value of the force threshold $\tilde{f}_c$.

We now discuss how parameter changes affect the location of the boundaries between the different dynamical regimes in Fig. 7 *c*. First, it is clear that increasing the basepairing energy ε_b, will shift both force thresholds, f_c and f^*, toward higher forces. Furthermore, from the above microscopic picture, it follows that the inward hopping rate k_{in} is proportional to the average loop density, while the outward hopping rate k_{out} decreases with the loop density. The average loop density, in turn, is affected by our energy parameters: with increasing ε_b, ε_ℓ, the average loop density decreases, and consequently the boundary $\tilde{f}_c(\nu)$ is shifted toward lower mutation densities, i.e., the sliding regime becomes more sensitive to mutations (this tendency is enhanced by the rising energetic cost for opening a mutation).

So far, we considered only mutations with binding energy equal to the original bases. Dropping this restriction leads to a sloped boundary $f^*(\nu)$ between the sliding and unraveling regimes, and also affects the slope of $\tilde{f}_c(\nu)$. Furthermore, we assumed above that all mutations are of a different type and bind only to their native binding partner. Without this assumption, bases belonging to different mutated basepairs can bind on encounter during the sliding phase. These basepairs have to be opened in the same way as during the waiting phase preceding sliding. When mutations are equidistant, this effect becomes particularly strong, leading to additional intervals of constant length, i.e., plateaus in the extension versus time-trace. Another important effect, caused both by variable spacing and energies of mutations, is that the hopping rates k_{in} and k_{out} become site-dependent, so that the random walks are effectively on a rugged-energy landscape (31,32).

Finally, we stress that the 2RW model is phenomenological and fails to describe certain features of the DNA dynamics. (For instance, our simple description has neglected correlations between subsequent hopping steps of an RW; see Supplementary Material.) Short-range correlations do not affect the long-time behavior, which may explain why our model describes the shape of the waiting-time distribution accurately (see Fig. 5). A more drastic approximation is that the 2RW model does not account for the time required to bring in new loops from the ends to a mutation deep inside the dsDNA. The fact that this time increases with the length of the DNA may be the cause for the waiting time to rise more rapidly with the system size than expected from the 2RW model (see Fig. 7).

CONCLUSIONS AND OUTLOOK

The basepairing dynamics in DNA and RNA molecules is only beginning to be explored. Here, we have shown that even the seemingly simple case of periodic DNA sequences displays rich behavior, which can be revealed by applying a shear force. Our main finding is that the microscopic dynamics of bulge-loop defects endows DNA with viscoelastic properties, which can be programmed into the sequence. Weak sequence disorder does not abolish these properties, but 1), introduces a delay, since all mutations have to be broken before DNA sliding begins, and 2), effectively narrows the viscoelastic force regime. The dynamics of mutation breaking is an interesting stochastic process, with main features that can be understood by considering a first-passage problem of two random walkers. Our theoretical study has led to several experimental ramifications. For instance, we predict that periodic or nearly periodic DNA responds to sudden stress by slowly relaxing its tension to a threshold value independent of the initial stress (provided the DNA is not too short). This stress relaxation process cannot occur for heterogeneous DNA. Furthermore, we predict that the relaxation velocity is inversely proportional to the DNA length, so that the timescale of the dynamics can be easily adjusted into the range of interest for a given experimental setup. We expect the existence of the different dynamical regimes shown in Fig. 7 *c* to be independent of our detailed model assumptions. As DNA slippage is directly linked to the production rate and mobility of bulge loops, single-molecule experiments on DNA sliding would test our basic understanding of basepairing dynamics in DNA.

The same properties, which make DNA uniquely suited for reliably storing genetic information while keeping it accessible, permit many applications in nanotechnology (5). For instance, dsDNA has been used as a reversible cross-linker in polymer networks to switch between different mechanical properties (7), and even DNA-only networks with specified topologies can be constructed, exploiting the specificity of the basepairing interaction (5). In other applications, short dsDNA molecules served as programmable force sensors (6) using the sequence-dependence of the mechanical rupture force, or DNA-based nanomachines were constructed on the basis of the DNA branch migration mechanism (33). Our results render several new applications for DNA in nanotechnology conceivable. For instance, complementary periodic ssDNAs could be used as self-tightening connections in nanostructures: once two such strands found each other, they will slide to maximize their overlap until the tension reaches a value f_c. Periodic or nearly periodic DNA could also serve as a viscoelastic crosslinker in polymer networks, which should lead to different material properties from those observed in Lin et al. (7). Similarly, DNA networks could also be endowed with viscoelastic properties, and (nearly) periodic DNA might even be useful as a programmable reference molecule for kinetic measurements. Of course, which of these and other possible applications will turn out to be useful in the end is unclear at the present stage. However, we feel that there is a clear potential that should be explored.

SUPPLEMENTARY MATERIALS

An online supplement to this article can be found by visiting BJ Online at http://www.biophysj.org.

REFERENCES

1. SantaLucia, J., Jr. 1998. A unified view of polymer, dumbbell, and oligonucleotide DNA nearest-neighbor thermodynamics. *Proc. Natl. Acad. Sci. USA.* 95:1460–1465.

2. Hagerman, P. J. 1990. Sequence-directed curvature of DNA. *Annu. Rev. Biochem.* 59:755–781.

3. Widom, J. 2001. Role of DNA sequence in nucleosome stability and dynamics. *Q. Rev. Biophys.* 34:269–324.

4. Rippe, K., P. H. von Hippel, and J. Langowski. 1995. Action at a distance: DNA-looping and initiation of transcription. *Trends Biochem. Sci.* 20:500–506.

5. Seeman, N. C. 2003. DNA in a material world. *Nature.* 421:427–431.

6. Albrecht, C., K. Blank, M. Lalic-Multhaler, S. Hirler, T. Mai, I. Gilbert, S. Schiffmann, T. Bayer, H. Clausen-Schaumann, and H. E. Gaub. 2003. DNA: a programmable force sensor. *Science.* 301:367–370.

7. Lin, D. C., B. Yurke, and N. A. Langrana. 2004. Mechanical properties of a reversible, DNA-crosslinked polyacrylamide hydrogel. *J. Biomech. Eng.* 126:104–110.

8. Bustamante, C., J. C. Macosko, and G. J. Wuite. 2000. Grabbing the cat by the tail: manipulating molecules one by one. *Nat. Rev. Mol. Cell Biol.* 1:130–136.

9. Clausen-Schaumann, H., M. Seitz, R. Krautbauer, and H. E. Gaub. 2000. Force spectroscopy with single bio-molecules. *Curr. Opin. Chem. Biol.* 4:524–530.

10. Merkel, R. 2001. Force spectroscopy on single passive biomolecules and single biomolecular bonds. *Phys. Rep.* 346:343–385.

11. Lavery, R., A. Lebrun, J.-F. Allemand, D. Bensimon, and V. Croquette. 2002. Structure and mechanics of single biomolecules: experiment and simulation. *J. Phys. Cond. Mater.* 14:R383–R414.

12. Bockelmann, U., P. Thomen, B. Essevaz-Roulet, V. Viasnoff, and F. Heslot. 2002. Unzipping DNA with optical tweezers: high sequence sensitivity and force flips. *Biophys. J.* 82:1537–1553.

13. Danilowicz, C., V. W. Coljee, C. Bouzigues, D. K. Lubensky, D. R. Nelson, and M. Prentiss. 2003. DNA unzipped under a constant force exhibits multiple metastable intermediates. *Proc. Natl. Acad. Sci. USA.* 100:1694–1699.

14. Altan-Bonnet, G., A. Libchaber, and O. Krichevsky. 2003. Bubble dynamics in double-stranded DNA. *Phys. Rev. Lett.* 90:138101.

15. Lubensky, D. K., and D. R. Nelson. 2002. Single molecule statistics and the polynucleotide unzipping transition. *Phys. Rev. E.* 65:031917.

16. Strunz, T., K. Oroszlan, R. Schäfer, and H.-J. Güntherodt. 1999. Dynamic force spectroscopy of single DNA molecules. *Proc. Natl. Acad. Sci. USA.* 96:11277–11282.

17. Pörschke, D. 1974. Model calculations on the kinetics of oligonucleotide double helix coil transitions. Evidence for a fast chain sliding reaction. *Biophys. Chem.* 2:83–96.

18. Neher, R. A., and U. Gerland. 2004. Dynamics of force-induced DNA-sliding. *Phys. Rev. Lett.* 93:198102.

19. Reddy, P. S., and D. E. Housman. 1997. The complex pathology of trinucleotide repeats. *Curr. Opin. Cell Biol.* 9:364–372.

20. Lovett, S. T. 2004. Encoded errors: mutations and rearrangements mediated by misalignment at repetitive DNA sequences. *Mol. Microbiol.* 52:1243–1253.

21. Hallatschek, O., E. Frey, and K. Kroy. 2005. Propagation and relaxation of tension in stiff polymers. *Phys. Rev. Lett.* 94:077804.

22. Smith, S. B., Y. Cui, and C. Bustamante. 1996. Overstretching B-DNA: the elastic response of individual double-stranded and single-stranded DNA molecules. *Science.* 271:795–799.

23. Flamm, C., W. Fontana, I. L. Hofacker, and P. Schuster. 2000. RNA folding at elementary step resolution. *RNA.* 6:325–338.

24. Craig, M. E., D. M. Crothers, and P. Doty. 1971. Relaxation kinetics of dimer formation by self-complementary oligonucleotides. *J. Mol. Biol.* 62:383–392.

25. Harlepp, S., H. Isambert, D. Chatenay, S. Harlepp, T. Marchal, J. Robert, J. F. Leger, A. Xayaphoummine, D. Isambert, and H. Chatenay. 2003. Probing complex RNA structures by mechanical force. *Eur. Phys. J. E.* 12:605–615.

26. de Gennes, P. G. 1971. Reptation of a polymer chain in the presence of fixed obstacles. *J. Chem. Phys.* 55:572–579.

27. Zener, C. 1956. Elasticity and Anelasticity of Metals. The University of Chicago Press, Chicago, IL.

28. Gardiner, C. W. 2004. Handbook of Stochastic Methods. Springer-Verlag, Berlin, Germany.

29. Schwarz, M., and D. Poland. 1975. Random walk with two interacting walkers. *J. Chem. Phys.* 63:557–568.

30. Anshelevich, V. V., A. V. Vologodskii, A. V. Lukashin, and M. D. Frank-Kamenetskii. 1984. Slow relaxational processes in the melting of linear biopolymers: a theory and its application to nucleic acids. *Biopolymers.* 23:39–58.

31. Derrida, B. 1983. Velocity and diffusion constant of a periodic one-dimensional hopping model. *J. Stat. Phys.* 31:433–450.

32. Kafri, Y., D. K. Lubensky, and D. R. Nelson. 2004. Dynamics of molecular motors and polymer translocation with sequence heterogeneity. *Biophys. J.* 86:3373–3391.

33. Simmel, F. C., and B. Yurke. 2002. A DNA-based molecular device switchable between three distinct mechanical states. *Appl. Phys. Lett.* 80:883–885.